JACS
JOURNAL OF THE AMERICAN CHEMICAL SOCIETY

COMMUNICATION

pubs.acs.org/JACS

^{1}H-Detected ^{13}C Photo-CIDNP as a Sensitivity Enhancement Tool in Solution NMR

Jung Ho Lee,[†] Ashok Sekhar,[†] and Silvia Cavagnero*[,†,‡]

[†]Biophysics Graduate Program and [‡]Department of Chemistry, University of Wisconsin, Madison, Wisconsin 53706, United States

Supporting Information

ABSTRACT: NMR is a powerful yet intrinsically insensitive technique. The applicability of NMR to chemical and biological systems would be substantially extended by new approaches going beyond current signal-to-noise capabilities. Here, we exploit the large enhancements arising from ^{13}C photochemically induced dynamic nuclear polarization (^{13}C photo-CIDNP) in solution to improve biomolecular NMR sensitivity in the context of heteronuclear correlation spectroscopy. The ^{13}C-PRINT pulse sequence presented here involves an initial ^{13}C nuclear spin polarization via photo-CIDNP followed by conversion to anti-phase coherence and transfer to ^{1}H for detection. We observe substantial enhancements, up to ≫200-fold, relative to the dark (laser off) experiment. Resonances of both side-chain and backbone CH pairs are enhanced for the three aromatic residues Trp, His, and Tyr, the σ^{32} peptide, and the drkN SH3 protein. The sensitivity of this experiment, defined as signal-to-noise per square root of unit time $(S/N)_t$, is unprecedented in the NMR polarization enhancement literature dealing with polypeptides in solution. Up to a 16-fold larger $(S/N)_t$ than for the ^{1}H−^{13}C SE-HSQC reference sequence is achieved, for the σ^{32} peptide. Data collection time is reduced up to 256-fold, highlighting the advantages of ^{1}H-detected ^{13}C photo-CIDNP in solution NMR.

NMR is an invaluable spectroscopic tool to probe residue-specific molecular properties such as dynamics, folding, and noncovalent interactions. To date, this technique has been largely exploited to study native and nonnative states of biomolecules in solution, including peptides, proteins, and nucleic acids.[1]

Due to either scarce sample solubility,[2] the need to maintain low concentrations to overcome competing processes (e.g., aggregation), or the intrinsically low abundance of the target species in the relevant physiological environment,[3] liquid-state biomolecular NMR samples are often rather dilute, requiring highly sensitive data collection. In addition, real-time kinetic studies of fast events by NMR impose a need for rapid and efficient data collection even in concentrated samples.[4,5]

NMR's low sensitivity stems from marginal nuclear polarization at thermal equilibrium. Enhanced polarization methods tackle this problem by perturbing the thermal equilibrium upon coupling nuclei to other highly polarized quantum states.[6] For instance, in dynamic nuclear polarization (DNP), unpaired electron polarization is transferred to nuclei.[7] Para-hydrogen reacts with unsaturated substrates to create ^{1}H-polarized molecules.[9] Nuclear polarization via coupling with rotational quantum states of methyl groups and entire small molecules leads to NMR signal enhancements by the Haupt effect[10] and hyperfine depolarization,[11] respectively. In addition, electron polarization of alkali metals leads to hyperpolarization of noble gases via optical pumping.[12] Despite the large signal enhancements attainable, substrates amenable to these approaches are confined to the solid-state or to small molecules in liquid solution. Promising DNP methods that polarize samples directly in the liquid state[13] or rely on the rapid thawing of prepolarized frozen solutions have proven effective for small molecules (e.g., urea, glucose)[14] and dipeptides.[15] Nevertheless, the harsh, rapid dissolution procedures necessary for some of these applications are generally not desirable for large biomolecules.

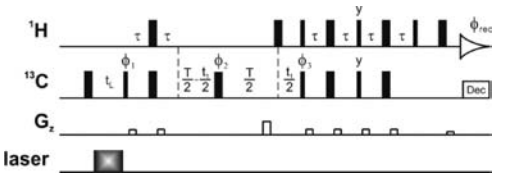

Figure 1. ^{13}C-PRINT NMR pulse sequence for ^{1}H-detected ^{13}C photo-CIDNP-enhanced data collection. T is the total evolution time in the indirect dimension (13 and 27 ms for side-chain and C$^{\alpha}$ carbons, respectively) for this constant-time sequence. τ was $1/4J_{CH}$ (1.6 ms), and t_L is the laser irradiation time. All pulses have x phase unless otherwise noted. ^{13}C decoupling during acquisition was performed by WURST140.[8] The phase cycling was $\phi_1 = y, -y$; $\phi_2 = y, y, -x, -x, -y, -y, x, x$; $\phi_{rec} = x, -x, -x, x$. Two-dimensional experiments were run in States-TPPI mode (i.e., phase shifting of ϕ_1, ϕ_3, ϕ_{rec} concurrent with sign inversion of the last z-gradient). The initial ^{13}C π pulse is used to constructively add emissive ^{13}C photo-CIDNP polarization to the pre-existing ^{13}C magnetization. In the case of absorptive ^{13}C photo-CIDNP polarization, the π pulse is omitted.

An alternative method, photochemically induced dynamic nuclear polarization (photo-CIDNP), offers considerable potential and opportunities, mostly unexplored to date,[5,16−18] as an NMR sensitivity enhancement tool for the study of both small and large biomolecules examined under mild solution conditions. According to the radical pair mechanism (RPM),[19] photo-CIDNP[20,21] proceeds via laser-triggered formation of a transient radical pair between oxidizable amino acids (typically Trp, His, and Tyr) and a light-absorbing oxidizing dye (often flavin mononucleotide, FMN). After laser irradiation, the photoexcited dye in its triplet state extracts an electron from a nearby residue, giving rise to a transient radical pair. Recombination rates back to the original species depend on the hyperfine coupling between the

Received: December 24, 2010
Published: May 06, 2011

   dx.doi.org/10.1021/ja111613c | J. Am. Chem. Soc. 2011, 133, 8062–8065

Table 1. $(S/N)_t$ Enhancements Obtained in Solution via ^{13}C-PRINT for Trp, His, Tyr, and the σ^{32} Peptide[a,b]

	samples									
	Trp		His		Tyr			σ^{32} peptide		
reference exp.	η2	α	ε1	α	δ1, δ2	ε1, ε2	α	η2	δ1	α
^{1}H-^{13}C SE-HSQC	11.8 ± 0.7	3.95 ± 0.03	10.4 ± 0.3	0.49 ± 0.02	6.7 ± 0.4	7.5 ± 0.4	2.9 ± 0.3	12 ± 1	6.9 ± 0.1	16 ± 1
^{13}C-PRINT dark	41 ± 2	22 ± 3	43 ± 4	2.2 ± 0.2	21 ± 2	38 ± 3	14 ± 1	≫200[c]	≫200[c]	220 ± 20
^{13}C-PRINT dark′[d]	27 ± 1	13.5 ± 0.6	36 ± 2	1.88 ± 0.07	16 ± 1	23 ± 2	11.7 ± 0.3	30 ± 2	27.1 ± 0.6	60 ± 1

[a] The t_L values giving rise to maximum signal under light conditions (see Figures 2, 3) were used for calculating the enhancements in this table. [b] All uncertainties were propagated considering the ±1 standard error in $(S/N)_t$ resulting from three independent measurements. [c] No explicit $(S/N)_t$ could be evaluated for these experiments because the dark spectrum lacked any detectable signal beyond the noise, even for prolonged data collection (64 transients). [d] The notation *dark′* denotes dark reference experiments with t_L set to 0 s.

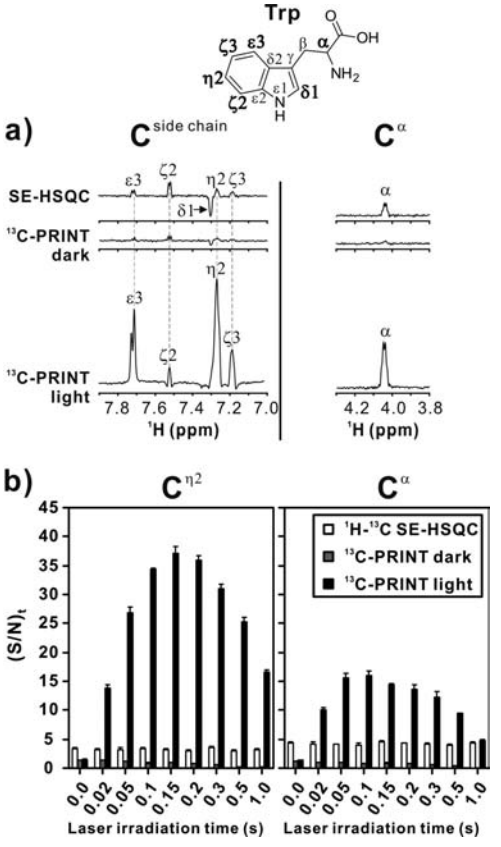

Figure 2. (a) One-dimensional ^{13}C-PRINT NMR spectra illustrating the ^{1}H-detected ^{13}C photo-CIDNP enhancements of 1.0 mM Trp in aqueous solution. A spectral window of 6000 Hz with 1000 complex points was used. The t_1 carbon chemical shift evolution was set to 0. The relaxation delay was set to 1.5 s in all experiments. Four transients and two steady-state scans were collected. The data shown in this panel were acquired with a laser irradiation time t_L corresponding to the maximum $(S/N)_t$ [see t_L dependence profiles in panel (b)]. Spectra were phased so that resonances resulting from emissive enhancements are positive. All the NMR data shown in this work were collected on a Varian INOVA 600 MHz spectrometer equipped with a triple resonance ^{1}H{^{13}C,^{15}N} triple axis gradient probe. (b) Dependence of ^{13}C photo-CIDNP enhancements on the laser irradiation time t_L. Experimental conditions and acquisition parameters other than t_L are as in panel (a). $(S/N)_t$, defined as $(S/N)/t^{1/2}$, was determined as described.[18] All measurements were carried out on three independent samples. Uncertainties are expressed as ±1 standard error of the mean. Note that an increase in t_L leads to a decrease in *dark* $(S/N)_t$ due to ^{13}C T_1 relaxation during laser irradiation.

unpaired electron and the surrounding nuclei. The effect of the hyperfine coupling can be highly nuclear-spin-state-dependent, resulting in the selectively faster recombination for one of the nuclear spin states (α or β, in case of spin-1/2 nuclei). This process leads to enrichment in the fast-recombining nuclear spins and is the key aspect of photo-CIDNP. The fraction of molecules bearing the nuclear spin state with slower recombination rate does not effectively contribute to the net polarization. In this case, the radical pairs are often sufficiently long-lived to dissociate and then undergo rapid paramagnetic nuclear relaxation, leading to thermally equilibrated spin populations at the applied field. All magnetically active nuclei in solvent-exposed oxidizable residues of polypeptides and proteins are potential photo-CIDNP candidates.

The heteronuclear photo-CIDNP sensitivity enhancement efforts carried out so far focused on the Trp indole ^{15}N−^{1}H bond pair, and exploited (a) ^{15}N CIDNP followed by ^{15}N→^{1}H nuclear polarization transfer,[16] (b) ^{1}H CIDNP followed by ^{1}H→^{15}N→^{1}H transfer,[16,17] (c) ^{1}H→^{15}N nuclear polarization transfer followed by ^{15}N CIDNP and ^{15}N→^{1}H transfer,[18] or a combination of (b) and (c).[18] While these studies led to promising enhancements, their applicability is limited by the fact that the ^{15}N−^{1}H pair in the Trp indole is the only viable probe. Furthermore, the Trp indole ^{15}N−^{1}H resonances tend to be poorly dispersed in nonnative proteins.[22]

Inspired by the established existence of ^{13}C photo-CIDNP,[23,24] the large enhancements achieved via ^{1}H-detected ^{15}N heteronuclear photo-CIDNP[16,18] and considering that there are many ^{13}C−^{1}H bond pairs in aromatic residues, we explored the potential of heteronuclear ^{1}H-detected ^{13}C photo-CIDNP. We show that this effect leads to large NMR sensitivity enhancements in several ^{13}C−^{1}H resonances of Trp, His, and Tyr, including both side-chain and backbone $^{13}C^{\alpha}$−^{1}H's. Thus, ^{13}C photo-CIDNP followed by polarization transfer to ^{1}H enables the highly sensitive detection of both side-chain and backbone resonances in amino acids, polypeptides, and proteins.

As shown in Figure 1, the ^{13}C photo-CIDNP-enhanced constant time reverse INEPT (^{13}C-PRINT) pulse sequence is designed to enhance ^{13}C polarization followed by transfer to ^{1}H for detection. In the case of emissive photo-CIDNP, the initial ^{13}C π pulse constructively adds ^{13}C longitudinal magnetization to ^{13}C-photo-CIDNP-induced polarization. The photo-CIDNP-inducing light beam, which was generated via a Spectra Physics 2017-AR in multiline mode with main lines at 488 and 514 nm, operating at 5.0 and 0.5−2.0 W for one- and two-dimensional (1D and 2D) experiments, respectively, was guided into the NMR sample tube inside the magnet via an optical fiber.[17,18] Uniformly ^{13}C, ^{15}N-enriched Trp, His, Tyr (1.0 mM each), the

dx.doi.org/10.1021/ja111613c | J. Am. Chem. Soc. 2011, 133, 8062–8065

N-terminal SH3 domain of the drk adaptor protein from *Drosophila* (drkN SH3, 0.3 mM), and the σ^{32} peptide (1.0 mM) bearing ^{13}C,^{15}N-Trp were used as model substrates. Unless otherwise stated, data were collected in the presence of 0.2 mM of FMN in 95% H_2O/5% D_2O adjusted to pH 7.0, at 24 °C. The chemically synthesized σ^{32} peptide (see primary structure in Figure 4) comprises the 132−144 residues of the *Escherichia coli* σ^{32} transcriptional regulator, with Leu_{135} replaced by ^{13}C,^{15}N-Trp.[25]

Figure 2 shows that $^{13}C-^{1}H$ photo-CIDNP leads to significant increases in signal-to-noise per unit time $(S/N)_t$ for free Trp under laser-on (*light*) conditions, relative to both laser-off (*dark*) conditions and to a reference sensitivity-enhanced pulse-field-gradient $^{1}H-^{13}C$ HSQC sequence[26] in constant-time mode[27] (denoted as $^{1}H-^{13}C$ SE-HSQC). The observed enhancements, relative to $^{1}H-^{13}C$ SE-HSQC, are 12- and 4-fold for $^{13}C^{\eta 2}-^{1}H$ and $^{13}C^{\alpha}-^{1}H$, respectively (Table 1). This result is particularly significant if one considers that $^{1}H-^{13}C$ SE-HSQC involves a full $^{1}H\rightarrow^{13}C\rightarrow^{1}H$ transfer, whereas ^{13}C-PRINT only entails a $^{13}C\rightarrow^{1}H$ transfer. Even larger enhancements (41- and 22-fold) are detected, relative to dark conditions. A second type of dark experiment, denoted as dark′, was also performed, with laser irradiation time (t_L) set to 0 to minimize unnecessary signal losses due to ^{13}C T_1 relaxation in the reference experiment. The observed Trp enhancements for $^{13}C^{\eta 2}-^{1}H$ and $^{13}C^{\alpha}-^{1}H$ relative to the dark′ experiments are 27 and 14-fold, respectively (Table 1). Figure 2b shows how $(S/N)_t$ varies upon increasing t_L. After the maximum enhancement is reached, a decrease in $(S/N)_t$ at long t_L is observed under light conditions, due to reduced sample photostability and ^{13}C T_1 relaxation, both of which counteract ^{13}C photo-CIDNP buildup. This profile shows the main drawback of photo-CIDNP, i.e., the need to properly modulate laser power and irradiation time to minimize photodegradation. Comparable photo-CIDNP enhancements are also found for His and Tyr (Figure 3, Table 1). ^{13}C,^{15}N-labeled Leu and Ser, on the other hand, experience no photo-CIDNP enhancement. Note that Tyr displays a significant C^{α} enhancement, while this effect is negligible for His. Small C^{β} ^{13}C-PRINT enhancements are also observed for Trp (data not shown). These C^{β} steady-state enhancements are smaller than in time-resolved CIDNP,[24] likely due to differences in the extent of cancellation effects.[21]

To address the method's applicability to larger biological systems, we first analyzed the σ^{32} model polypeptide, as shown in Figure 4. Interestingly, even larger enhancements than in the case of free Trp are observed for the σ^{32} peptide. ^{13}C-PRINT yields 16-fold larger $(S/N)_t$ than $^{1}H-^{13}C$ SE-HSQC for C^{α}, which is 4-fold larger than the enhancement observed for free Trp (Table 1). Photo-CIDNP enhancement patterns are also different for the side chain ^{13}C's of free Trp and the σ^{32} peptide's Trp. Specifically, a dramatic enhancement is observed for $^{13}C^{\delta 1}$ of the σ^{32} peptide Trp while a negligible effect is detected for the corresponding nucleus of free Trp (Figures 2, 4 and S1 (Supporting Information [SI]) and Table 1). Therefore, ^{13}C photo-CIDNP enhancement patterns can be sensitive to the surrounding chemical environment.

To illustrate the power of ^{13}C photo-CIDNP in cases where high resolution is critical, 2D ^{13}C-PRINT data were collected for the σ^{32} peptide (Figure 4b). Mild laser irradiation (power = 0.5W, t_L = 0.1 s) was employed in this case to optimize sample photostability (<5% degradation) during data collection. Significant enhancements are evident here too (Figure 4b). A comparison between Figures 4b and S1, S2 [SI] illustrates how $(S/N)_t$ is maximized, in the case of emissive photo-CIDNP (e.g., see Trp $^{13}C^{\varepsilon 3}$, $^{13}C^{\eta 2}$), by retaining the initial ^{13}C π pulse.

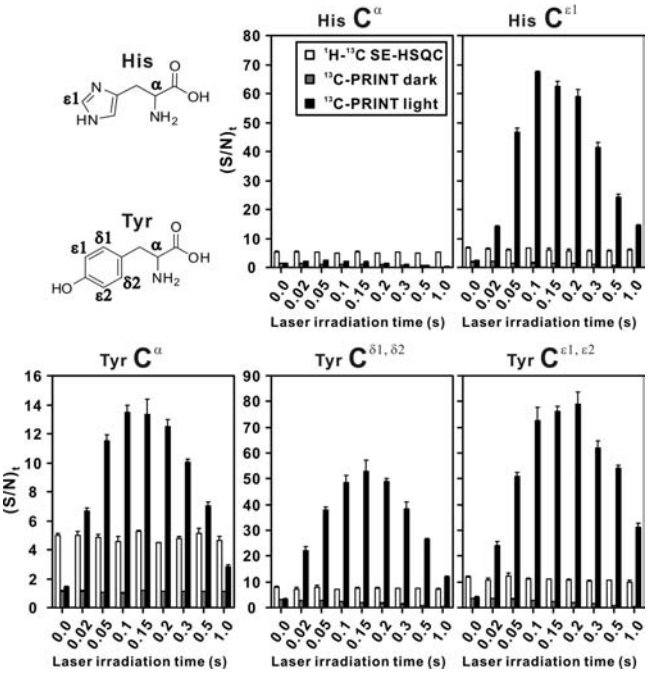

Figure 3. Laser irradiation time dependence of photo-CIDNP enhancements of His and Tyr via ^{13}C-PRINT. Experimental parameters and error analysis are as in Figure 2. The initial ^{13}C π pulse was omitted for the data collection on Tyr C^{α} because the photo-CIDNP enhancement is absorptive.

Finally, we collected 2D ^{13}C-PRINT data on drkN SH3, a protein that populates both native and unfolded states in slow exchange on the NMR chemical shift time scale (Figure S3 [SI]). $(S/N)_t$ enhancements of up to 2.4-fold relative to $^{1}H-^{13}C$ SE-HSQC were observed for the Trp_{36} and Tyr_{52} $^{1}H-^{13}C^{\alpha}$ pairs in the unfolded state. Moderate enhancements (1.7-fold) were also observed for the partially solvent-exposed Trp_{36} in the native state. The above experiments illustrate that ^{13}C-PRINT is an extremely sensitive tool to probe amino acid, peptide, and protein backbone conformation.

Comparisons between ^{13}C-PRINT enhancements of amino acids, peptide, and protein (Figures 2, 4 and S3 [SI]) show different relative intensities and signs. We ascribe these variations to a combination of (a) the greater extent of exchange and recombination cancellation expected for amino acids, relative to proteins, and (b) the different hyperfine constants arising from changes in electronic distribution of the different species, likely due to differences in primary structure, conformation, and protonation state of the radical cation within the transient radical ion pair.[21]

In summary, this work demonstrates the power of ^{13}C photo-CIDNP in heteronuclear correlation NMR. Indeed, ^{1}H-detected ^{13}C photo-CIDNP leads to sensitivity enhancement for both side-chain and backbone CH pairs in amino acids, peptides, and proteins in solution. The σ^{32} peptide sensitivity enhancement, up to 16-fold over SE-HSQC, reduces data collection time up to 256-fold and highlights the promise of this approach. Noteworthy are $^{13}C^{\alpha}-^{1}H$ enhancements as these nuclei are robust reporters of backbone secondary structure. While ^{13}C-PRINT is tailored to enhance resonances from specific solvent-exposed residues (Tyr, Trp, and His), recent advances suggest that in the future it may be possible to transfer photo-CIDNP-enhanced C^{α} and side-chain C magnetization to other nearby nuclei via NOE.[28] We anticipate that the ^{1}H-detected ^{13}C photo-CIDNP method will prove useful to study both equilibrium biological processes in dilute solutions and kinetic time courses demanding rapid data collection.

dx.doi.org/10.1021/ja111613c |*J. Am. Chem. Soc.* 2011, 133, 8062–8065

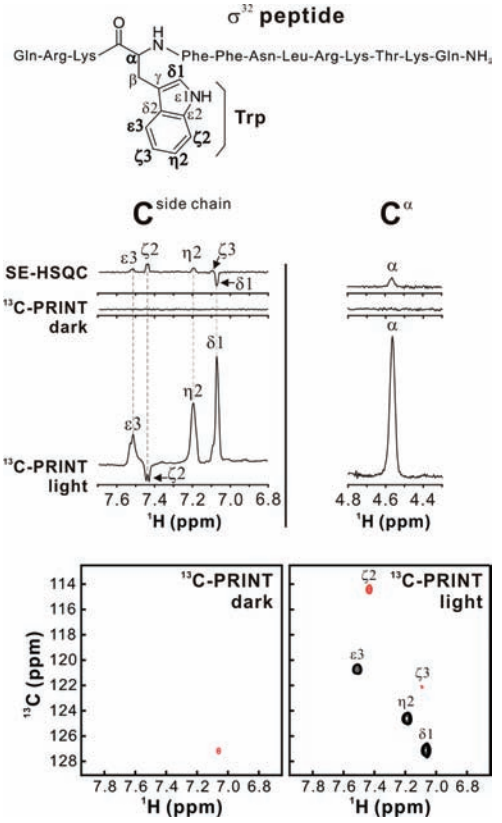

Figure 4. (a) One-dimensional NMR spectra for the ^{1}H-detected ^{13}C photo-CIDNP enhancement of the σ^{32} peptide. Experimental procedures are as in Figure 2. (b) Two-dimensional dark and light ^{13}C-PRINT spectra of the σ^{32} peptide. Two-dimensional data were collected according to States-TPPI with 32 increments and 1 scan per increment. Sweep widths of 6000 and 4000 Hz were employed, for the direct and indirect dimensions, respectively. Black and red contours denote positive and negative resonances, respectively. Emissive ^{13}C photo-CIDNP enhancements are detected for $C^{\delta 1}$, $C^{\varepsilon 3}$, and $C^{\eta 2}$, while absorptive enhancements are observed for $C^{\zeta 2}$ and $C^{\zeta 3}$. Note that emissive enhancements are phased to be positive.

■ ASSOCIATED CONTENT

Supporting Information. 2D ^{13}C-PRINT data on Trp, σ^{32} peptide (with no initial ^{13}C π pulse), and drkN SH3. This material is available free of charge via the Internet at http://pubs.acs.org.

■ AUTHOR INFORMATION

Corresponding Author
cavagnero@chem.wisc.edu

■ ACKNOWLEDGMENT

We are grateful to Alexandra Yurkovskaya, Lewis Kay, Charles Fry, and Milo Westler for helpful discussions, to Robert Shanks for technical assistance, and to Julie Forman-Kay for donating the drkN SH3 plasmid. This research was funded by the National Institute of Health Grant R21AI088551.

■ REFERENCES

(1) (a) Wright, P. E.; Dyson, H. J. *Curr. Opin. Struct. Biol.* **2009**, *19*, 31. (b) Dyson, H. J.; Wright, P. E. *Chem. Rev.* **2004**, *104*, 3607. (c) Gardner, K. H.; Kay, L. E. *Annu. Rev. Biophys. Biomol. Struct.* **1998**, *27*, 357. (d) Farrow, N. A.; Muhandiram, R.; Singer, A. U.; Pascal, S. M.; Kay, C. M.; Gish, G.; Shoelson, S. E.; Pawson, T.; Formankay, J. D.; Kay, L. E. *Biochemistry* **1994**, *33*, 5984.

(2) (a) Kurt, N.; Rajagopalan, S.; Cavagnero, S. *J. Mol. Biol.* **2006**, *355*, 809. (b) Kurt, N.; Cavagnero, S. *Biophys. J.* **2008**, *94*, L48.

(3) (a) Rajagopalan, S.; Chow, C.; Raghunathan, V.; Fry, C. G.; Cavagnero, S. *J. Biomol. NMR* **2004**, *29*, 505. (b) Bakke, C. K.; Jungbauer, L. M.; Cavagnero, S. *Protein Expression Purif.* **2006**, *45*, 381.

(4) (a) Frydman, L.; Scherf, T.; Lupulescu, A. *Proc. Natl. Acad. Sci. U.S.A.* **2002**, *99*, 15858. (b) Gal, M.; Schanda, P.; Brutscher, B.; Frydman, L. *J. Am. Chem. Soc.* **2007**, *129*, 1372. (c) Giraudeau, P.; Shrot, Y.; Frydman, L. *J. Am. Chem. Soc.* **2009**, *131*, 13902.

(5) Shapira, B.; Morris, E.; Muszkat, K. A.; Frydman, L. *J. Am. Chem. Soc.* **2004**, *126*, 11756.

(6) Köckenberger, W.; Matysik, J. In *Encyclopedia of Spectroscopy and Spectrometry*; Lindon, J. C., Ed.; Elsevier: Oxford, 2010; p 963.

(7) (a) Overhauser, A. W. *Phys. Rev.* **1953**, *92*, 411. (b) Carver, T. R.; Slichter, C. P. *Phys. Rev.* **1953**, *92*, 212. (c) Special issue on DNP. *Phys. Chem. Chem. Phys.* **2010**, *12* (22).

(8) Kupce, E.; Freeman, R. *J. Magn. Reson., Ser. A* **1995**, *115*, 273.

(9) Natterer, J.; Bargon, J. *Prog. Nucl. Magn. Reson. Spectrosc.* **1997**, *31*, 293.

(10) Haupt, J. *Phys. Lett. A* **1972**, *38*, 389.

(11) (a) Rakitzis, T. P.; Samartzis, P. C.; Toomes, R. L.; Kitsopoulos, T. N.; Brown, A.; Balint-Kurti, G. G.; Vasyutinskii, O. S.; Beswick, J. A. *Science* **2003**, *300*, 1936. (b) Van Brunt, R. J.; Zare, R. N. *J. Chem. Phys.* **1968**, *48*, 4304.

(12) (a) Navon, G.; Song, Y.; Room, T.; Appelt, S.; Taylor, R. E.; Pines, A. *Science* **1996**, *271*, 1848. (b) Goodson, B. M. *J. Magn. Reson.* **2002**, *155*, 157.

(13) (a) Reese, M.; Turke, M. T.; Tkach, I.; Parigi, G.; Luchinat, C.; Marquardsen, T.; Tavernier, A.; Hofer, P.; Engelke, F.; Griesinger, C.; Bennati, M. *J. Am. Chem. Soc.* **2009**, *131*, 15086. (b) Lingwood, M. D.; Han, S. G. *J. Magn. Reson.* **2009**, *201*, 137. (c) Loening, N. M.; Rosay, M.; Weis, V.; Griffin, R. G. *J. Am. Chem. Soc.* **2002**, *124*, 8808.

(14) (a) Ardenkjaer-Larsen, J. H.; Fridlund, B.; Gram, A.; Hansson, G.; Hansson, L.; Lerche, M. H.; Servin, R.; Thaning, M.; Golman, K. *Proc. Natl. Acad. Sci. U.S.A.* **2003**, *100*, 10158. (b) Joo, C. G.; Casey, A.; Turner, C. J.; Griffin, R. G. *J. Am. Chem. Soc.* **2009**, *131*, 12.

(15) Vasos, P. R.; Comment, A.; Sarkar, R.; Ahuja, P.; Jannin, S.; Ansermet, J. P.; Konter, J. A.; Hautle, P.; van den Brandt, B.; Bodenhausen, G. *Proc. Natl. Acad. Sci. U.S.A.* **2009**, *106*, 18469.

(16) Lyon, C. E.; Jones, J. A.; Redfield, C.; Dobson, C. M.; Hore, P. J. *J. Am. Chem. Soc.* **1999**, *121*, 6505.

(17) Sekhar, A.; Cavagnero, S. *J. Phys. Chem. B* **2009**, *113*, 8310.

(18) Sekhar, A.; Cavagnero, S. *J. Magn. Reson.* **2009**, *200*, 207.

(19) (a) Kaptein, R.; Oosterhoff, J. L. *Chem. Phys. Lett.* **1969**, *4*, 195. (b) Closs, G. L.; Closs, L. E. *J. Am. Chem. Soc.* **1969**, *91*, 4550.

(20) (a) Bargon, J.; Fischer, H.; Johnson, U. *Z. Naturforsch., A: Phys. Sci.* **1967**, *22*, 1551. (b) Ward, H. R.; Lawler, R. G. *J. Am. Chem. Soc.* **1967**, *89*, 5518. (c) Kaptein, R.; Dijkstra, K.; Nicolay, K. *Nature* **1978**, *274*, 293. (d) Closs, G. L.; Miller, R. J.; Redwine, O. D. *Acc. Chem. Res.* **1985**, *18*, 196.

(21) Hore, P. J.; Broadhurst, R. W. *Prog. Nucl. Magn. Reson. Spectrosc.* **1993**, *25*, 345.

(22) Schlorb, C.; Mensch, S.; Richter, C.; Schwalbe, H. *J. Am. Chem. Soc.* **2006**, *128*, 1802.

(23) (a) Lippmaa, E.; Pehk, T.; Buchachenko, A. L.; Rykov, S. V. *Chem. Phys. Lett.* **1970**, *5*, 521. (b) Thamarath, S. S.; Heberle, J.; Hore, P. J.; Kottke, T.; Matysik, J. *J. Am. Chem. Soc.* **2010**, *132*, 15542.

(24) Kiryutin, A. S.; Morozova, O. B.; Kuhn, L. T.; Yurkovskaya, A. V.; Hore, P. J. *J. Phys. Chem. B* **2007**, *111*, 11221.

(25) McCarty, J. S.; Rudiger, S.; Schonfeld, H. J.; Schneider-Mergener, J.; Nakahigashi, K.; Yura, T.; Bukau, B. *J. Mol. Biol.* **1996**, *256*, 829.

(26) Kay, L. E.; Keifer, P.; Saarinen, T. *J. Am. Chem. Soc.* **1992**, *114*, 10663.

(27) Cavanagh, J. *Protein NMR Spectroscopy: Principles and Practice*; Academic Press: New York, 2007.

(28) Mok, K. H.; Kuhn, L. T.; Goez, M.; Day, I. J.; Lin, J. C.; Andersen, N. H.; Hore, P. J. *Nature* **2007**, *447*, 106.